

# Comprehensive Analysis of lincRNA-Related ceRNA Network in Glioblastoma

**Guangdong Liu**

Mudanjiang Medical University

**Danian Liu**

Mudanjiang Medical University

**Jingjing Huang**

Mudanjiang Medical University

**Jianxin Li**

People's Hospital of Jiaozuo City

**Chuang Wang**

Mudanjiang Medical University

**Guangyao Liu**

Mudanjiang Medical University

**Shiqiang Ge**

Mudanjiang Medical University

**Haidong Gong** (✉ [149585079@qq.com](mailto:149585079@qq.com))

Mudanjiang Medical University <https://orcid.org/0000-0003-2002-5179>

---

## Research article

**Keywords:** Glioblastoma, ceRNA, lincRNA, weighted gene co-expression network analysis, prognostic model

**Posted Date:** October 8th, 2020

**DOI:** <https://doi.org/10.21203/rs.3.rs-86624/v1>

**License:**  This work is licensed under a Creative Commons Attribution 4.0 International License.

[Read Full License](#)

---

**Version of Record:** A version of this preprint was published on January 26th, 2021. See the published version at <https://doi.org/10.1186/s12885-021-07817-5>.

# Abstract

## Background

Long intergenic non-coding RNAs (lincRNAs) are capable of regulating several tumours, while competitive endogenous RNA (ceRNA) networks are of great significance in revealing the biological mechanism of tumours. Currently, there is a dearth of studies on the ceRNA network of lincRNAs in glioblastoma (GBM), which we aimed to assess in the present study.

## Methods

We obtained GBM and normal brain tissue samples from TCGA, GTEx, and GEO databases, and performed weighted gene co-expression network analysis and differential expression analysis on all lincRNA and mRNA data. Subsequently, we predicted the interaction between lincRNAs, miRNAs, and target mRNAs. Univariate and multivariate Cox regression analyses were performed on the mRNAs using CGGA data, and a Cox proportional hazards regression model was constructed.

## Results

According to the Cox model, we assembled a ceRNA network consisting of 23 lincRNAs, 14 miRNAs, and 13 mRNAs. Gene Set Enrichment Analysis was carried out on four lincRNAs with obvious differential expressions and relatively few studies in GBM.

## Conclusion

We identified four lincRNAs that have the most research values for GBM and obtained the ceRNA network. Our research is expected to facilitate in-depth understanding and study of the molecular mechanism of GBM, and provide new insights into targeted therapy and prognosis of the tumour.

# Background

Glioblastoma (GBM) is the most aggressive and destructive primary malignant central nervous system tumour [1]. At present, the most established treatment protocol for this tumour involves curative surgery and adjuvant radiotherapy combined with temozolomide; however, its prognosis is still very poor, and the average survival time of patients is approximately 2 years [2]. Moreover, various treatment methods affect normal brain tissue, and the quality of life of patients does not significantly improve afterwards. Therefore, an in-depth study of the molecular mechanism of GBM occurrence and development, while exploring possible therapeutic targets, may prove beneficial for the diagnosis and treatment of the tumour.

Although approximately 90% of genes in the human genome can be transcribed, only approximately 2% of the genes are protein coding, and non-coding RNAs account for most of the remainder [3]. Long non-coding RNAs (lncRNAs) contain >200 nucleotides and have no protein coding function. They are mainly

transcribed from different regions of the genome by RNA polymerase II, and have been shown to be closely related to cancer [4,5]. The tissue specificity of lincRNA expression has been reported to be higher than that of mRNA expression, which applies even in pathological conditions such as cancer [6]. Long intergenic non-coding RNA (lincRNA) is a type of lincRNA that does not overlap with exons of protein-coding genes and other non-lincRNA genes, and participates in many important biological processes [7,8]. Cancer-related lincRNAs may be targeted to provide new ways for cancer diagnosis and treatment [9]. linc-ROR is a tumour promoter, which mainly participates in tumour cell proliferation, apoptosis, invasion, angiogenesis, and cancer stem cell generation by regulating target genes [10]. *NEAT1* is a p53-regulated lincRNA, which plays a key role in cancer occurrence [11]. lincRNA-p21 plays an important role in regulating TAM function in tumour microenvironments, and can be used as a new cancer treatment target for macrophage infiltration [12]. In general, molecular mechanisms related to lincRNA in tumours have important research value.

A competitive endogenous RNA (ceRNA) network is the interaction between lincRNAs, miRNAs, and mRNAs that constitutes a complex regulatory network systems, which has extensive functions in the human genome and plays a significant role in cancer [13]. It has been reported that linc-ROR can be used as the ceRNA of miR-145 to regulate the proliferation, invasion, and tumourigenicity of pancreatic cancer cells [14]. Further, a study has demonstrated that lincRNA-HOTAIR is highly expressed in a variety of tumour tissues and cells, and is associated with tumour metastasis and poor prognosis. Additionally, its related ceRNA network has been shown to play a role in the progression of kidney cancer [15]. However, to our knowledge, there is currently no study on ceRNA network related to lincRNA in GBM. Therefore, in this study, we comprehensively analysed the GBM data retrieved from The Cancer Genome Atlas (TCGA), National Center for Biotechnology Information (NCBI), Gene Expression Omnibus (GEO), Chinese Glioma Genome Atlas (CGGA), and Genotype Tissue Expression (GTEx) databases. We used weighted gene co-expression network analysis (WGCNA) and differential analysis to screen key lincRNAs, construct lincRNA-related ceRNA networks in GBM, and obtain a prognostic model. We believe this study provides a basis for further studies on the molecular mechanism of GBM and exploration of new therapeutic targets.

## Methods

### Data acquisition and pre-processing

We obtained RNA-Seq data of 165 GBM samples and 1,029 normal brain tissue samples from the TCGA and GTEx databases, respectively, using the UCSC Xena Browser (<https://xena.ucsc.edu/>). Further, the mRNA-seq and clinical data of 693 glioma samples were retrieved from CGGA (<http://cgga.org.cn/>), from which 248 GBM samples were selected for this study. Among the selected samples, 236 patients had survival information, while 198 had all clinical information. Additionally, we retrieved GSE50161 (comprising 34 GBM and 13 normal samples; platform: Affymetrix-GPL570) and GSE134783 (comprising 71 GBM samples; platform: Affymetrix-GPL570) from the GEO database (<https://www.ncbi.nlm.nih.gov/geo/>).

The IDs of all samples were transformed into gene symbols based on GENCODE (<https://www.genecodegenes.org/human/>). The RNA-seq data fetched from TCGA and GTEx were collated and merged, and the expression matrices of mRNA and lincRNA were obtained. We also combined and normalised the GEO data and obtained the mRNA expression matrix.

### **Construction of weighted gene co-expression network**

Using the combined data of TCGA and GTEx, a weighted gene co-expression network was constructed for lincRNA and mRNA. Based on the mRNA of the GEO combined data, a weighted gene co-expression network was constructed. WGCNA R software package [16] was used to build a co-expression network to mine key modules related to GBM. First, a hierarchical cluster analysis was performed to check the heterogeneity of the samples. Subsequently, according to the scale-free topological standard, we chose the appropriate soft threshold power ( $\beta$ ) to construct a weighted adjacency matrix and convert the adjacency relationship into a topological overlap matrix. Finally, we obtained the gene module, estimated the relationship between the module and trait, determined the module related to GBM, and showed the correlation between GBM and key gene modules, using a scatter plot.

### **Screening of differentially expressed genes**

We used the Limma R package [17] to screen the differentially expressed lincRNA (DElincRNA) between the GBM patients and control group from the combined data of TCGA and GTEx.

Differential expression analysis was performed on the mRNA data in the TCGA and GTEx combined data and GEO combined data, and the two selected differential genes were combined to obtain differentially expressed mRNA (DEmRNA) ( $P < 0.05$ , and  $|\log_2 FC| \geq 1$ ).

### **Preliminary construction of ceRNA network**

The most relevant modules to GBM were selected and analysed with DElincRNA to screen for overlapping lincRNA. Further, miRcode (<http://www.mircode.org/>) was used to predict miRNA, and the miRNA target mRNA was predicted using miRDB (<http://www.mirdb.org/>), miRTarBase (<http://mirtarbase.mbc.nctu.edu.tw/>), and TargetScan (<http://www.targetscan.org/>). The predicted mRNA, key module and DEmRNA were analysed to obtain overlapping mRNA. Additionally, Cytoscape 3.7.2 software was used to visualise the ceRNA network.

### **Gene function and pathway enrichment analysis**

We used the clusterProfiler R package [18] for Gene Ontology (GO) analysis and Kyoto Encyclopedia of Genes and Genomes (KEGG) enrichment analysis. GO is used to describe gene function, and KEGG is used to obtain possible pathways. Further, the GOplot R package [19] was used to visualise the GO term or KEGG approach (adjusted  $p < 0.05$ ).

### **Construction of Cox regression model**

Univariate COX regression analysis was performed on the CGGA data, using the Survival R software package, to evaluate the effect of mRNA expression on the survival time of GBM patients. Additionally, we performed multivariate COX regression analysis, constructed a multivariate Cox regression model, and identified the corresponding coefficients of GBM prognostic features. Further, we calculated the risk score to predict survival time, dividing the samples into high-risk and low-risk groups, with the median as the critical value. The "predict ()" function was used to calculate the risk score:  $\text{risk score} = h_0(t) \cdot \exp(\beta_1 x_1 + \beta_2 x_2 + \dots + \beta_n x_n)$ . The correlation between the prognostic characteristics of patients and overall survival rate was then calculated through univariate and multivariate Cox regression analyses of clinical factors related to overall survival. Finally, the R package survivalROC was used to draw the receiver operating characteristic curve and calculate the area under the curve (AUC).

### **ceRNA network in GBM**

According to the mRNA obtained by multivariate Cox regression analysis, we screened the corresponding miRNA and lincRNA and reconstructed the ceRNA network.

### **Gene Set Enrichment Analysis (GSEA)**

GSEA software was used to analyse the RNA-seq data of lincRNA retrieved from the CGGA database. According to the median of lincRNA expression, the samples were divided into high and low expression groups. Statistical significance was set at  $p < 0.05$ . A set of genes "c2. cp. kegg. v7.2. symbols. gmt" was retrieved from the Molecular Signature Database (MSigDB, <http://software.broadinstitute.org/gsea/msigdb/index.jsp>) and selected as the reference gene set.

## **Results**

### **WGCNA identifies key modules**

We combined GTEx and TCGA data to construct a co-expression network for all lincRNAs, using the R package 'WGCNA', and confirmed that the  $\beta$  value in the network was 4 (Figure 1A). Further, the dynamic tree cutting method was used to generate co-expression modules, and the closely related modules were merged into larger modules. Finally, 19 modules were generated in the lincRNA co-expression network (Figure 1B). The module eigengenes (MEs) of the turquoise module had the strongest correlation with GBM traits (Figure 1C). Figure 1D shows the correlation between gene significance and module membership in the turquoise module, which was considered a key module containing 2,206 lincRNAs.

We also constructed the co-expression networks of all mRNAs for GTEx and TCGA combined data and GEO combined data, comprising 20,270 and 14,807 mRNAs, respectively. In the mRNA co-expression networks of the two sets of data,  $\beta$  values were 8 and 4 (Figure 2A and Figure 3A), and 22 and 21 modules were generated (Figure 2B and Figure 3B), respectively. In the combined GTEx and TCGA data, the MEs of the blue and dark green modules have the strongest correlations with the tumour and normal traits, respectively (Figure 2C). The blue and dark green modules were considered key modules,

comprising 7,736 mRNAs. In the GEO data, Figure 3C shows that the MEs of the blue and turquoise modules (comprising 8,022 mRNAs) have the strongest correlations with the tumour and normal traits, respectively. Figures 2D-E and 3D-E show the correlation between gene significance and module membership.

### **Identification of differentially expressed lincRNAs (DE lincRNAs) and mRNAs (DEmRNAs)**

We identified DELincRNAs and DEmRNAs from the GTEx and TCGA combined data, including 163 up-regulated lincRNAs, 176 down-regulated lincRNAs, 2,953 up-regulated mRNAs, and 2,932 down-regulated mRNAs. From the GEO data, 2,434 up-regulated and 1,995 down-regulated mRNAs were identified. The two groups of mRNAs were then comprehensively analysed to obtain overlapping 1,040 down-regulated mRNAs and 1,358 up-regulated mRNAs. Finally, 339 DELincRNAs and 2,398 DEmRNAs were identified.

### **Preliminary construction of ceRNA network**

Through WGCNA analysis of lincRNAs, we obtained 2,206 lincRNAs in the turquoise module and then integrated the analysis with 339 DELincRNAs to obtain 251 overlapping lincRNAs. Further, using the miRcode online tool, 251 lincRNAs were used to predict miRNAs. Additionally, using the miRDB, TargetScan, and miRTarBase datasets, the predicted miRNAs were used to obtain the corresponding mRNAs. By analysing the predicted mRNAs and DEmRNAs, we obtained 111 mRNAs (24 down-regulated and 87 up-regulated mRNAs). The predicted miRNAs and 251 lincRNAs were analysed using the 111 mRNAs, and 25 lincRNAs and 30 miRNAs were finally obtained. Subsequently, we used Cytoscape version 3.7.2 software to build a lincRNA-miRNA-mRNA ceRNA network (Figure 4).

### **Functional Enrichment Analysis**

A functional enrichment analysis was performed on the 111 mRNAs obtained previously. The biological processes of enrichment were mainly cell cycle, epithelial cell proliferation, ossification, and sex differentiation (Figure 5A). The cellular components were concentrated in the transcription factor, protein kinase, and serine/threonine protein kinase complexes (Figure 5 B). Enriched molecular function was mainly involved in DNA-binding transcription activator activity, RNA polymerase II-specific core promoter binding, and HMG box domain binding (Figure 5 C). KEGG pathway analysis showed that the genes were associated with cellular senescence, cell cycle, multiple cancers, miRNA in cancer, and TGF-beta signalling pathway (Figure 5 D).

### **Construction of prognostic models**

Among the CGGA GBM samples, complete survival information was available for 236 samples, and all clinical information was available for 198 samples. Univariate Cox regression analysis was performed on the 111 mRNAs previously obtained, and 27 mRNAs related to survival time were obtained ( $p < 0.05$ ) (Figure 6A). Multivariate Cox analysis was performed using 27 mRNAs, and a Cox proportional hazards regression model of GBM patients containing 13 mRNAs was constructed (Figure 6B). Based on the median risk score, all patients were divided into two groups (high-risk and low-risk groups). Figure 6C

shows the survival status, survival time, and mRNA expression levels of patients. Survival analysis showed that patients in the low-risk group survived longer than those in the high-risk group ( $p < 0.001$ ) (Figure 6D). The univariate Cox regression analysis showed that recurrence ( $p = 0.004$ ), isocitrate dehydrogenase (IDH) mutation ( $p = 0.009$ ), 1p19q codeletion ( $p = 0.014$ ), and risk score ( $p = 0.001$ ) were predictors (Figure 6E). Moreover, multivariate Cox regression analysis confirmed that recurrence ( $p = 0.002$ ) and risk score ( $p < 0.001$ ) were independent risk factors (Figure 6F). The risk score and recurrence AUCs of the nomogram were 0.668 and 0.663, respectively (Figure 6G).

### ceRNA network in GBM

The 13 mRNAs obtained through the previous multivariate COX regression analysis, as well as the 14 miRNAs and 23 lincRNAs interacting with them, were used to construct the final ceRNA network (Figure 7).

### GSEA reveals the close relationship between lincRNA and GBM

Using  $|\log_2FC| \geq 2$  as a condition to screen 23 kinds of lincRNA, we obtained seven of them: *MALAT1*, *MEG3*, *NEAT1*, *MIR7-3HG*, *FAM95B1*, *EPB41L4A-AS1*, and *AC125494.1*. Among them, extensive research has been conducted on *MALAT1* and *NEAT1*. Thus, we selected *MEG3*, *MIR7-3HG*, *FAM95B1*, and *EPB41L4A-AS1* in 248 CGGA samples for GSEA. As shown in Figure 8, the GSEA results revealed that these lincRNAs were closely related to cancer. *MEG3* showed potential effects on prostate cancer, colorectal cancer, and cancer pathways (Figure 8A), *MIR7-3HG* demonstrated potential role in small cell lung cancer, prostate cancer, and cancer pathways (Figure 8B), *FAM95B1* was closely related to endometrial cancer, non-small cell lung cancer, renal cell carcinoma, and MTOR signalling pathway (Figure 8C), while *EPB41L4A-AS1* was associated with small cell lung cancer, prostate cancer, and JAK/STAT signalling pathway (Figure 8D). *AC125494.1* is not found in the CGGA data.

## Discussion

GBM, which is the most common type of glioma, accounts for about 15% of all brain tumours. It has been reported that there are about three GBM patients per 100,000 people, and the average survival time of patients is only approximately 12–18 months. The 5-year and 10-year survival rates are approximately 5.5% and 2.9%, respectively [20,21]. The low recovery rate and poor survival time of GBM patients may be related to the lack of efficient therapeutic targets. Therefore, it is of great significance to find new biomolecular markers and therapeutic targets of GBM. Currently, many scholars and research institutions focus on the role of non-coding RNAs in tumours, and several molecules have been significantly associated. Studies have shown that many lincRNAs can act as oncogenes or tumour suppressor genes in cancer. In recent years, ceRNA network-related research has gained intense attention. In a ceRNA network, lincRNAs can competitively bind miRNAs to regulate the expression of target mRNAs. Additionally, several studies have shown that ceRNA network is closely related to the occurrence and development of cancer and may be valuable in predicting the prognosis of patients.

In this study, we used WGCNA to find key modules related to GBM and combined differentially expressed genes for analysis. Based on the lincRNA-miRNA-mRNA interaction, a ceRNA network of GBM patients was preliminarily constructed, and 111 mRNAs in the network were functionally enriched. The results showed that these mRNAs have potential roles in cell cycle, cell proliferation, various cancers, miRNA in cancer, DNA-binding transcriptional activator activity, TGF- $\beta$  signalling pathway, transcription factor complex, RNA polymerase II specificity, etc. Further, univariate Cox regression and multivariate Cox regression analyses were used to construct a Cox proportional hazards regression model with 13 key genes: *CDK6*, *FAM84B*, *FBLIM1*, *FJX1*, *GNB5*, *HOXA3*, *MLEC*, *PDXK*, *SOX11*, *SPRY4*, *TBPL1*, *TRIB2*, and *WEE1*. We calculated the risk score of patients, and verified that the prognostic model is highly accurate. In addition, the nomogram based on the risk score has the highest AUC value. Finally, 13 mRNAs, 14 miRNAs, and 23 lincRNAs were used to construct a ceRNA network. We selected four lincRNAs, including *MEG3*, *MIR7-3HG*, *FAM95B1*, and *EPB41L4A-AS1*, and predicted their functions using the GSEA software. Our previous study showed that these four lincRNAs were significantly under-expressed in GBM. These lincRNAs were shown to be closely related to a variety of cancers. Among them, *MEG3* and *MIR7-3HG* are related to cancer pathways, while these two and *EPB41L4A-AS1* all regulate the JAK/STAT signalling pathway.

*MALAT1* and *NEAT1* have been widely studied non-coding RNAs, and some studies have demonstrated that they have clear correlations with various cancers such as hepatocellular carcinoma and lung cancer [22-25]. It has also been reported that *MALAT1* can be used as ceRNA of miR-199a to promote the expression of *ZHX1*, which in turn can regulate the proliferation of GBM cells [26]. The ceRNA effect between *NEAT1* and miR-194-5p is related to the angiogenesis of glioma [27].

*MEG3*, also known as gene trap locus 2, is an imprinted gene located at 14q32 [28]. It is a new type of tumour suppressor that plays a role in various tumours, such as ovarian and bladder cancers [29,30]. Studies have shown that *MEG3* is under-expressed in gliomas, and its over-expression has a significant inhibitory effect on the proliferation and migration of glioma cells, while promoting its apoptosis and autophagy, and inhibiting the PI3K/AKT/mTOR signalling pathway [31,32]. *MEG3* can act as a ceRNA for miR-19a, thereby exerting an inhibitory effect on glioma [33]. The present study also predicted that *MEG3* is potentially valuable in multiple tumours and cancer pathways.

According to previous reports, *MIR7-3HG* is associated with tumour progression and is highly expressed in endometrial cancer. Bioinformatics analysis by Wang et al. showed that its high expression in breast cancer is significantly related to the survival time of patients [34,35]. It has also been reported that this gene can be used as ceRNA to up-regulate the expression of *PEG10* by sponged miR-27a-3p, and thus plays a role in retinoblastoma [36]. *EPB41L4A-AS1*, located in the 5q22.2 region of the human genome, is an induced gene of p53 and pGC-1 $\alpha$ , can regulate glycolysis and glutamine metabolism, and plays an important role in cancer metabolic reprogramming [37]. It is highly expressed in colorectal cancer tissues and is involved in the proliferation, invasion, and migration of colorectal cancer cells [38]. Additionally, *FAM95B1* has been shown to be associated with thyroid cancer [39]. Limitations of our study include the

lack of cell or animal experiments and its retrospective nature. Subsequently, we hope to verify our results by conducting cell-based experiments.

## Conclusion

Conclusively, in this study, we constructed the lincRNA-miRNA-mRNA ceRNA network of GBM, which may be involved in its molecular regulation, and identified four lincRNAs with potential roles in the tumour. To our knowledge, three of these lincRNAs, namely *MIR7-3HG*, *FAM95B1*, and *EPB41L4A-AS1*, are novel potential therapeutic targets for GBM, as there are no previous related studies. Further, we created a prognostic model containing 13 genes, which may serve as a reliable prognostic indicator of GBM. Limitations of our study include the lack of cell or animal experiments and its retrospective nature. Subsequently, we hope to verify our results by conducting cell-based experiments. However, the present study is expected to facilitate in-depth understanding and study the molecular mechanism of GBM, and provide new insights into targeted therapy and prognosis of tumours.

## Abbreviations

LincRNA: Long intergenic non-coding RNA; ceRNA: competitive endogenous RNA; GBM: glioblastoma; TCGA: The Cancer Genome Atlas; NCBI: National Center for Biotechnology Information; GEO: Gene Expression Omnibus; CGGA: Chinese Glioma Genome Atlas; GTEx: Genotype Tissue Expression; WGCNA: weighted gene co-expression network analysis; GO: Gene Ontology; KEGG: Kyoto Encyclopedia of Genes and Genomes; GSEA: Gene Set Enrichment Analysis.

## Declarations

### Authors' contributions

Guangdong Liu, Haidong Gong and Danian Liu were involved in the concept and design of the study. Guangdong Liu and Haidong Gong drafted the manuscript. All authors participated in acquisition, analysis and interpretation of the data; revised the manuscript; and read and approved the final version.

### Funding

This study was funded by the Mudanjiang Medical University Graduate Innovation Fund of China (grant number 2019YJSCX-05MY).

### Availability of data and materials

The data comes from TCGA, GTEx, GEO, CGGA databases, which are all public open platforms.

### Ethics approval and consent to participate

Not applicable.

## Consent for publication

Not applicable.

## Competing interests

None.

## Author details

<sup>1</sup>Department of Neurosurgery, Hongqi Hospital affiliated to Mudanjiang Medical University, MuDanJiang, China. <sup>2</sup>Department of Neurology, Hongqi Hospital affiliated to Mudanjiang Medical University, MuDanJiang, China. <sup>3</sup>Department of Infectious Diseases, Hongqi Hospital affiliated to Mudanjiang Medical University, MuDanJiang, China. <sup>4</sup>Department of Neurosurgery, Jiaozuo People's Hospital, JiaoZuo, China.

## ORCID

Haidong Gong <https://orcid.org/0000-0003-2002-5179>

## References

1. Louis DN, Perry A, Reifenberger G, von Deimling A, Figarella-Branger D, Cavenee WK, Ohgaki H, Wiestler OD, Kleihues P, Ellison DW. The 2016 world health organization classification of tumors of the central nervous system: A summary. *Acta Neuropathol* 2016, 131(6):803-820.
2. Tanaka S, Louis DN, Curry WT, Batchelor TT, Dietrich J. Diagnostic and therapeutic avenues for glioblastoma: no longer a dead end? *Nat Rev Clin Oncol* 2013, 10(1):14-26.
3. Djebali S, Davis CA, Merkel A, Dobin A, Lassmann T, Mortazavi A, Tanzer A, Lagarde J, Lin W, Schlesinger F, et al: Landscape of transcription in human cells. *Nature* 2012, 489(7414):101-108.
4. Batista Pedro J, Chang Howard Y. Long noncoding RNAs: cellular address codes in development and disease. *Cell* 2013, 152(6):1298-1307.
5. Zhang HM, Zhu JK. Emerging roles of RNA processing factors in regulating long non-coding RNAs. *RNA Biol* 2014, 11(7):793-797.
6. Brunner AL, Beck AH, Edris B, Sweeney RT, Zhu SX, Li R, Montgomery K, Varma S, Gilks T, Guo X, et al: Transcriptional profiling of long non-coding RNAs and novel transcribed regions across a diverse panel of archived human cancers. *Genome biology* 2012, 13(8):R75.
7. Derrien T, Johnson R, Bussotti G, Tanzer A, Djebali S, Tilgner H, Guernec G, Martin D, Merkel A, Knowles DG, et al: The GENCODE v7 catalog of human long noncoding RNAs: Analysis of their gene structure, evolution, and expression. *Genome Res* 2012, 22(9):1775-1789.
8. Ulitsky I, Bartel DP. lincRNAs: Genomics, Evolution, and Mechanisms. *Cell* 2013, 154(1):26-46.

9. Tsai MC, Spitale RC, Chang HY. Long intergenic noncoding RNAs: New links in cancer progression. *Cancer Res* 2011, 71(1):3-7.
10. Pan Y, Li C, Chen J, Zhang K, Chu X, Wang R, Chen L. The Emerging Roles of Long Noncoding RNA ROR (lincRNA-ROR) and its Possible Mechanisms in Human Cancers. *Cell Physiol Biochem* 2016, 40(1-2):219-229.
11. Mello SS, Sinow C, Raj N, Mazur PK, Biegging-Rolett K, Broz DK, Imam JFC, Vogel H, Wood LD, Sage J, et al: Neat1 is a p53-inducible lincRNA essential for transformation suppression. *Genes Dev* 2017, 31(11):1095-1108.
12. Zhou LN, Tian Y, Guo F, Yu B, Li J, Xu H, Su Z. LincRNA-p21 knockdown reversed tumor-associated macrophages function by promoting MDM2 to antagonize\* p53 activation and alleviate breast cancer development. *Cancer Immunol Immunother* 2020, 69(5):835-846.
13. Salmena L, Poliseno L, Tay Y, Kats L, Pandolfi Pier P. A ceRNA hypothesis: the Rosetta stone of a hidden RNA language? *Cell* 2011, 146(3):353-358.
14. Gao S, Wang P, Hua YQ, Xi H, Meng Z, Liu T, Chen Z, Liu L. ROR functions as a ceRNA to regulate Nanog expression by sponging miR-145 and predicts poor prognosis in pancreatic cancer. *Oncotarget* 2015, 7(2):1608-1618.
15. Loewen G, Zhuo Y, Zhuang Y, Jayawickramarajah J, Shan B. lincRNA HOTAIR as a novel promoter of cancer progression. *Journal of cancer research updates* 2014, 3(3):134-140.
16. Langfelder P, Horvath S. WGCNA: an R package for weighted correlation network analysis. *BMC Bioinformatics* 2008, 9:559.
17. Ritchie ME, Phipson B, Wu D, Hu Y, Law CW, Shi W, Smyth GK. limma powers differential expression analyses for RNA-sequencing and microarray studies. *Nucleic Acids Res* 2015, 43(7):e47.
18. Yu GC, Wang LG, Han YY, He QY. ClusterProfiler: an R package for comparing biological themes among gene clusters. *Omics : a journal of integrative biology* 2012, 16(5):284-287.
19. Walter W, Sánchez-Cabo F, Ricote M. GOplot: an R package for visually combining expression data with functional analysis. *Bioinformatics (Oxford, England)* 2015, 31(17):2912-2914.
20. Ostrom QT, Gittleman H, Stetson L, Virk SM, Barnholtz-Sloan JS. Epidemiology of Gliomas. In: *Current Understanding and Treatment of Gliomas*. Volume 163, edn. Edited by Raizer J, Parsa A. Cham: Springer International Publishing; 2015: 1-14.
21. Ostrom QT, Gittleman H, Liao P, Vecchione-Koval T, Wolinsky Y, Kruchko C, Barnholtz-Sloan JS. CBTRUS Statistical Report: Primary brain and other central nervous system tumors diagnosed in the United States in 2010–2014. *Neuro-Oncology* 2017, 19(suppl\_5):v1-v88.
22. Peng NF, He JR, Li JD, Huang H, Huang W, Liao Y, Zhu S. Long noncoding RNA MALAT1 inhibits the apoptosis and autophagy of hepatocellular carcinoma cell by targeting the microRNA-146a/PI3K/Akt/mTOR axis. *Cancer Cell International* 2020, 20(1):165.
23. Zhu LY, Yang NH, Li CC, Liu G, Pan W, Li X. Long noncoding RNA NEAT1 promotes cell proliferation, migration, and invasion in hepatocellular carcinoma through interacting with miR-384. *J Cell Biochem* 2019, 120(2):1997-2006.

24. Song J, Su ZZ, Shen QM.: Long non-coding RNA MALAT1 regulates proliferation, apoptosis, migration and invasion via miR-374b-5p/SRSF7 axis in non-small cell lung cancer. *European review for medical and pharmacological sciences* 2020, 24(4):1853-1862.
25. Zang FR, Rao YQ, Zhu XH, Wu Z, Jiang H. Shikonin suppresses NEAT1 and Akt signaling in treating paclitaxel-resistant non-small cell of lung cancer. *Molecular medicine (Cambridge, Mass)* 2020, 26(1):28.
26. Liao KM, Lin YY, Gao WZ, Xiao Z, Medina R, Dmitriev P, Cui J, Zhuang Z, Zhao X, Qiu Y, et al: Blocking lncRNA MALAT1/miR-199a/ZHX1 axis inhibits glioblastoma proliferation and progression. *Molecular therapy Nucleic acids* 2019, 18:388-399.
27. Wang CL, Chen YX, Wang Y, Liu X, Liu Y, Li Y, Chen H, Fan C, Wu D, Yang J. Inhibition of COX-2, mPGES-1 and CYP4A by isoliquiritigenin blocks the angiogenic Akt signaling in glioma through ceRNA effect of miR-194-5p and lncRNA NEAT1. *Journal of experimental & clinical cancer research : CR* 2019, 38(1):371.
28. Benetatos L, Vartholomatos G, Hatzimichael E. MEG3 imprinted gene contribution in tumorigenesis. *International journal of cancer* 2011, 129(4):773-779.
29. Buttarelli M, De Donato M, Raspaglio G, Babini G, Ciucci A, Martinelli E, Baccaro P, Pasciuto T, Fagotti A, Scambia G, et al: Clinical value of lncrna MEG3 in high-grade serous ovarian cancer. *Cancers* 2020, 12(4):966.
30. Fan XR, Huang HF, Ji ZG, Mao QJTCR. Long non-coding RNA MEG3 functions as a competing endogenous RNA of miR-93 to regulate bladder cancer progression via PI3K/AKT/mTOR pathway. *2020 2020*, 9(3):1678-1688.
31. Zhao HK, Wang X, Feng XY, Li X, Pan L, Liu J, Wang F, Yuan Z, Yang L, Yu J, et al: Long non-coding RNA MEG3 regulates proliferation, apoptosis, and autophagy and is associated with prognosis in glioma. *Journal of Neuro-Oncology* 2018, 140(2):281-288.
32. Xu DH, Chi GN, Zhao CH, Li DY. Long noncoding RNA MEG3 inhibits proliferation and migration but induces autophagy by regulation of Sirt7 and PI3K/AKT/mTOR pathway in glioma cells. *2019*, 120(5):7516-7526.
33. Qin N, Tong GF, Sun LW, Xu XL. Long noncoding RNA MEG3 suppresses glioma cell proliferation, migration, and invasion by acting as a competing endogenous RNA of miR-19a. *Oncology research* 2017, 25(9):1471-1478.
34. Dong PX, Xiong Y, Yue JM, Xu D, Ihira K, Konno Y, Kobayashi N, Todo Y, Watari H. Long noncoding RNA NEAT1 drives aggressive endometrial cancer progression via miR-361-regulated networks involving STAT3 and tumor microenvironment-related genes. *Journal of experimental & clinical cancer research : CR* 2019, 38(1):295.
35. Wang JJ, Huang YQ, Song W, Li YF, Wang H, Wang WJ, Huang M. Comprehensive analysis of the lncRNA-associated competing endogenous RNA network in breast cancer. *Oncology reports* 2019, 42(6):2572-2582.

36. Ding FK, Jiang K, Sheng YJ, Li C, Zhu H. LncRNA MIR7-3HG executes a positive role in retinoblastoma progression via modulating miR-27a-3p/PEG10 axis. *Experimental Eye Research* 2020, 193:107960.
37. Liao MJ, Liao WJ, Xu NH, Li B, Liu F, Zhang S, Wang Y, Wang S, Zhu Y, Chen D, et al: LncRNA EPB41L4-AS1 regulates glycolysis and glutaminolysis by mediating nucleolar translocation of HDAC2. *EBioMedicine* 2019, 41:200-213.
38. Bin J, Nie S, Tang Z, Kang A, Fu Z, Hu Y, Liao Q, Xiong W, Zhou Y, Tang Y, et al: Long noncoding RNA EPB41L4-AS1 functions as an oncogene by regulating the Rho/ROCK pathway in colorectal cancer. *Journal of cellular physiology* 2020.
39. Li N, Cui MM, Yu P, Li Q. Correlations of lncRNAs with cervical lymph node metastasis and prognosis of papillary thyroid carcinoma. *Onco Targets Ther* 2019, 12:1269-1278.

## Figures

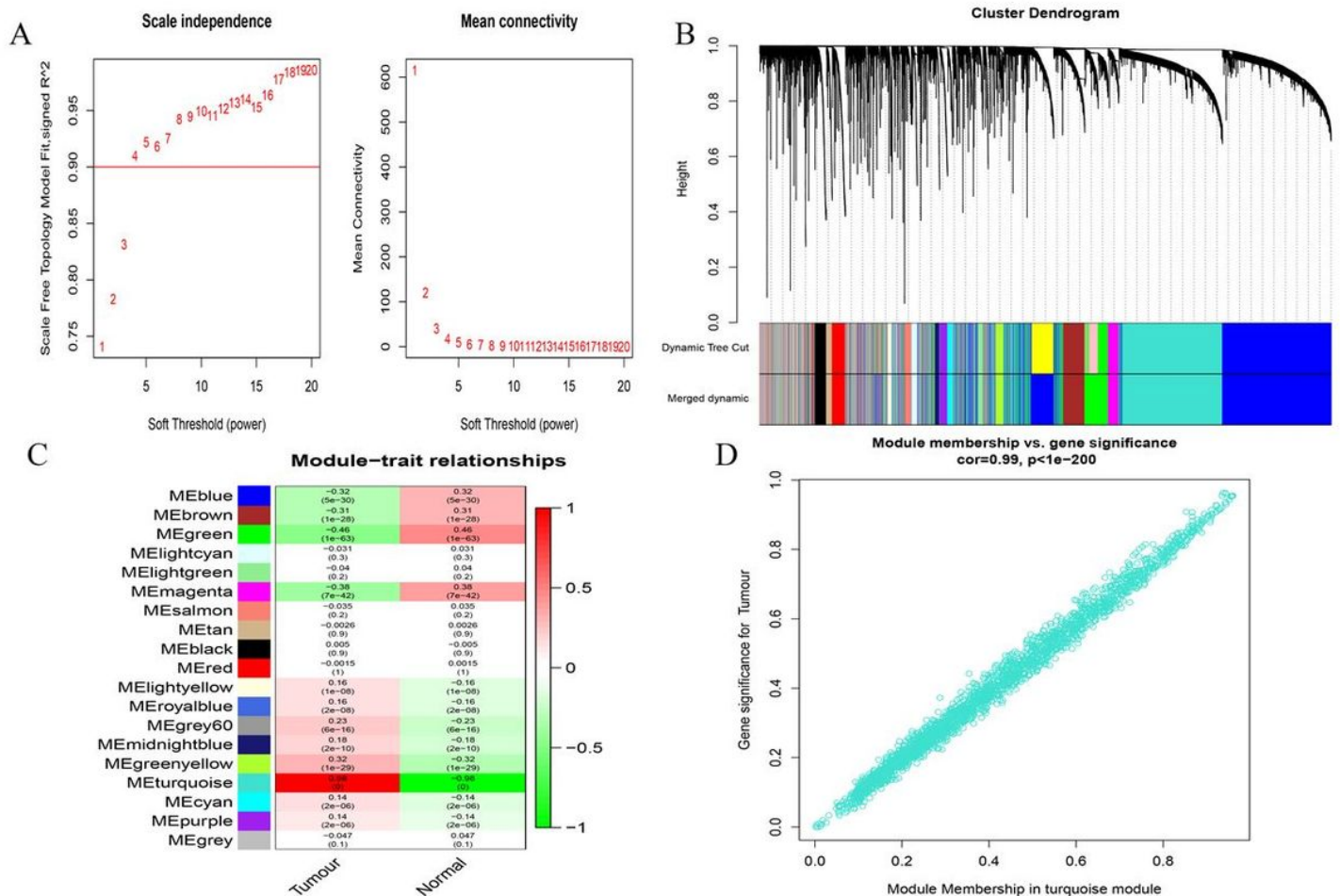


**Figure 1**

Identification of lincRNAs modules highly related to traits. A, Determination of soft-thresholding power in the lincRNAs WGCNA. Left: Analysis of the scale-free fit index for various soft-thresholding powers ( $\beta$ ).

Right: Analysis of the mean connectivity for various soft-thresholding powers. B, Cluster dendrogram of all lincRNA in the co-expression network. C, Module-trait associations of lincRNAs were evaluated by correlations between MEs and clinical traits. D, The correlation between GS and MM in the turquoise module.

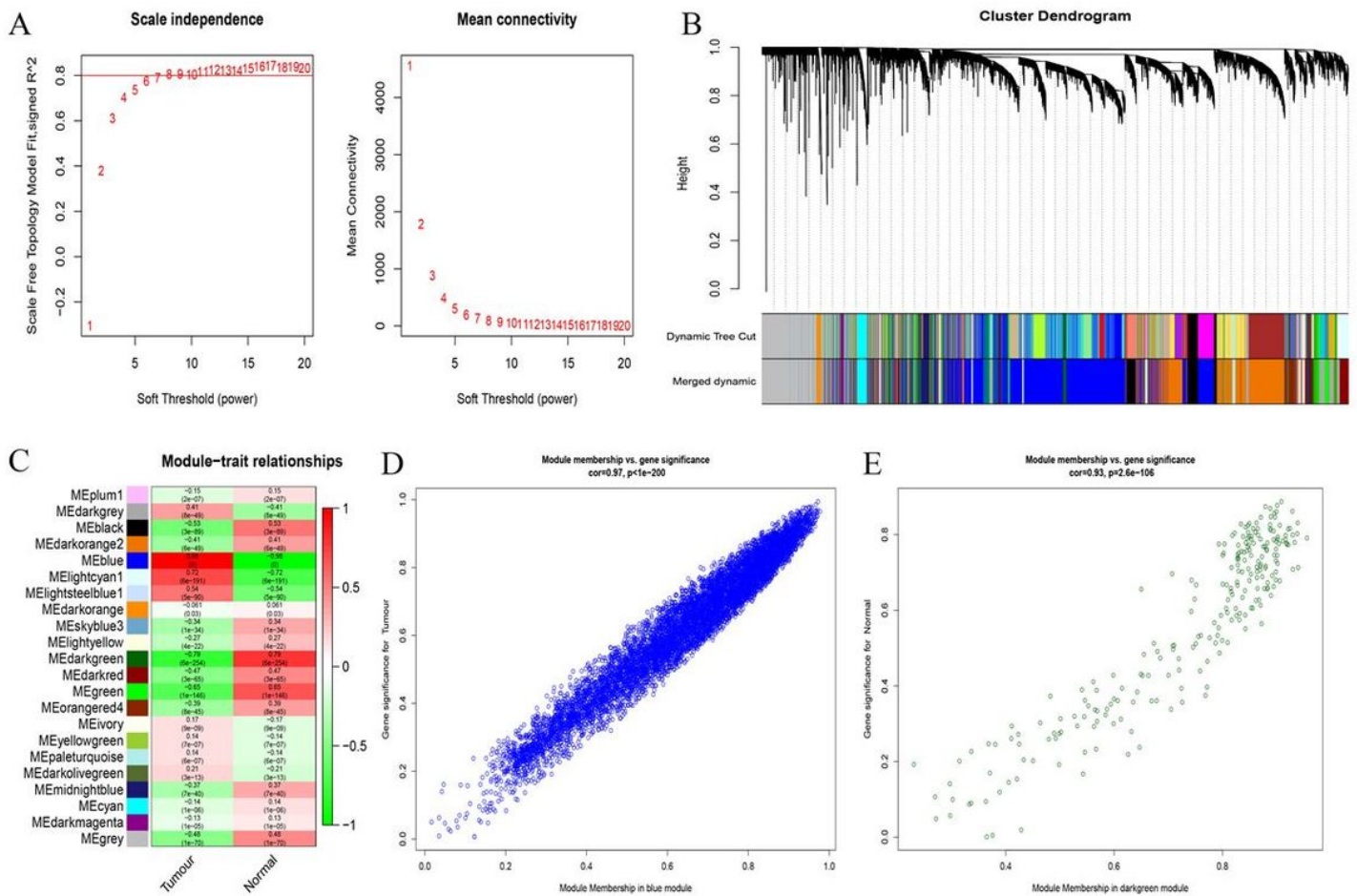


**Figure 2**

Identification of mRNAs modules highly related to traits in the combined data of TCGA and GTEx. A, Determination of soft-thresholding power. B, Cluster dendrogram of all mRNA in the co-expression network. C, The correlation between modules and traits were displayed. D, The correlation between GS and MM in the blue and darkgreen modules.

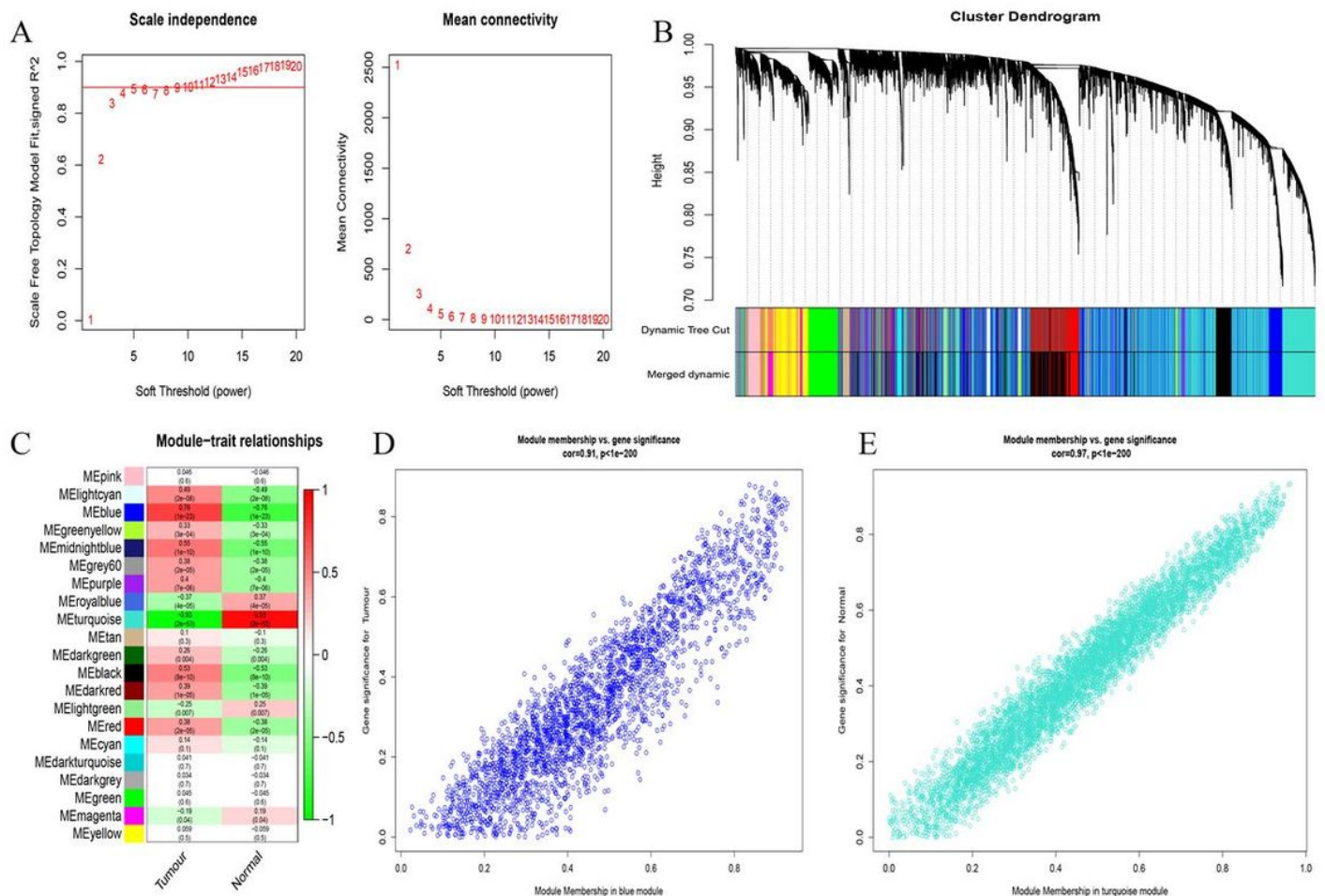


**Figure 3**

Identification of mRNAs modules highly related to traits in the combined data of GEO. A, Determination of soft-thresholding power. B, Cluster dendrogram of all mRNA in the co-expression network. C, The correlation between modules and traits were displayed. D, The correlation between GS and MM in the blue and turquoise modules.



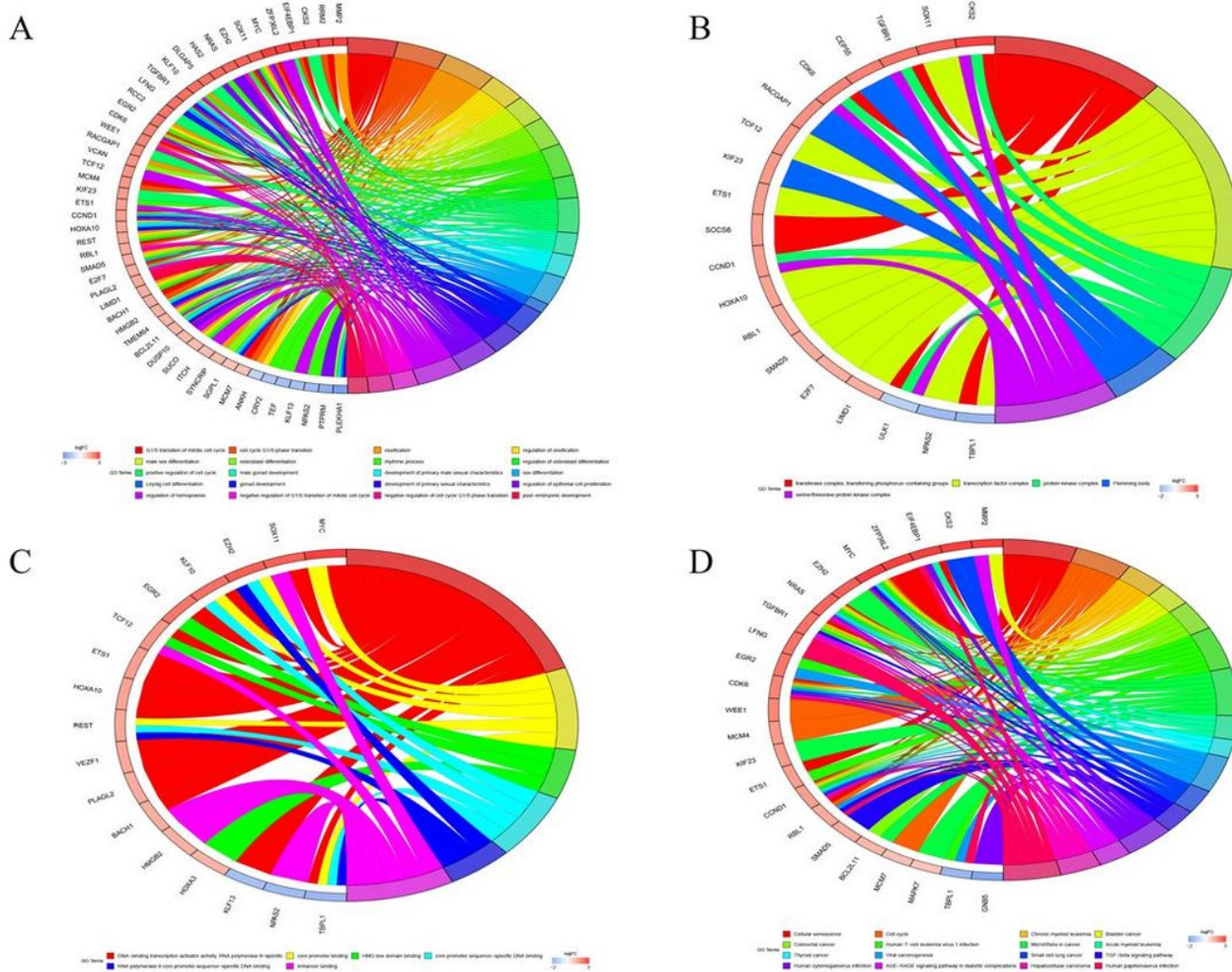


**Figure 5**

GO and KEGG analysis. A, The relationship between genes and GO terms of biological process. B, The relationship between genes and GO terms of cellular component. C, The relationship between genes and GO terms of molecular function. D, Chord plot indicates the relationship between genes and KEGG pathways. GO, Gene Ontology; KEGG, Kyoto Encyclopedia of Genes and Genomes.

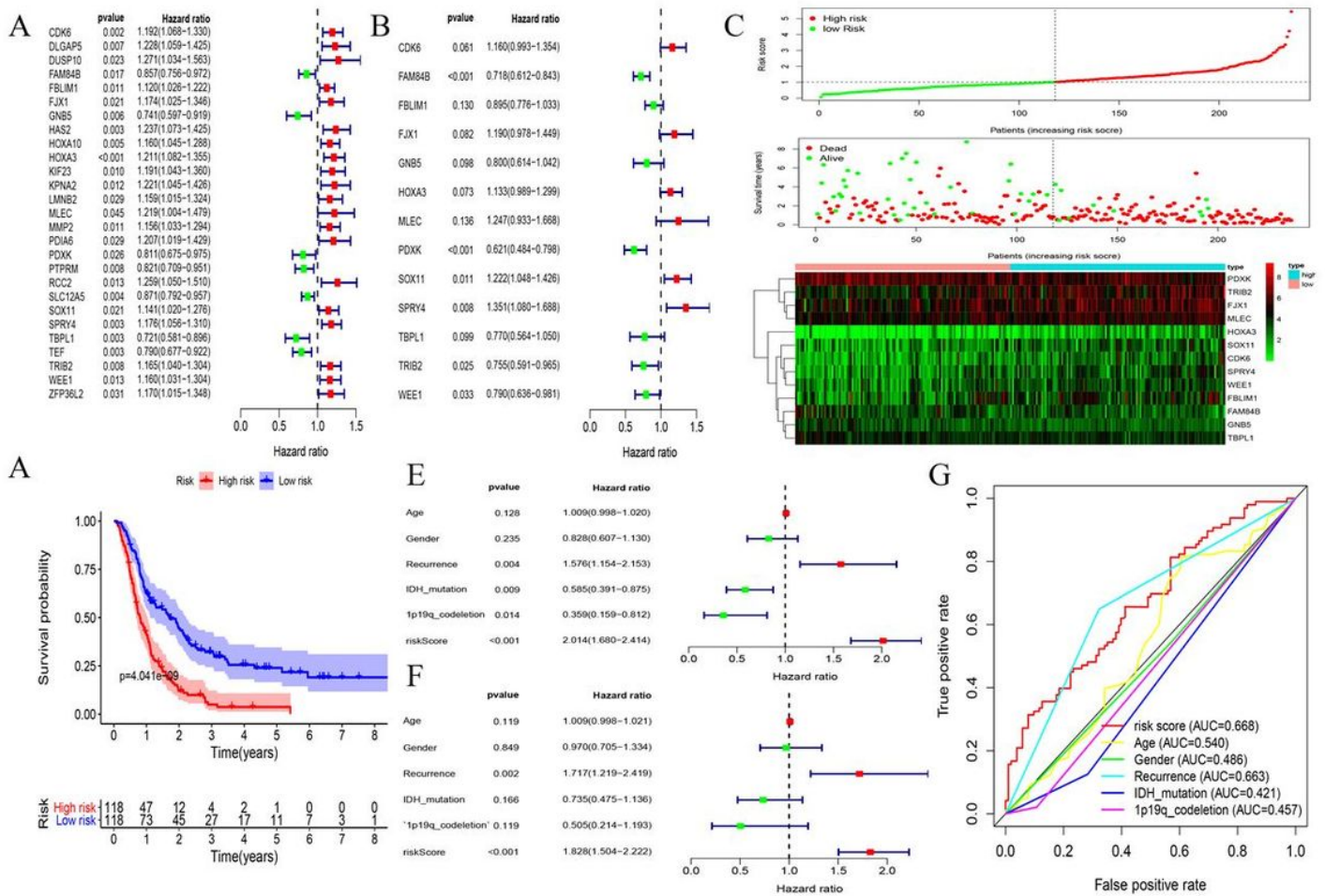


**Figure 6**

13-lincRNA prognosis model establishment and verification. A-B, Univariate Cox regression analysis and multivariate Cox regression analysis were used to construct prognostic models. C, Correlation between the prognostic signature and the overall survival of patients. The distribution of risk scores (upper), survival time (middle) and lincRNA expression levels (below). The black dotted lines represent the median risk score cut-off dividing patients into high- and low-risk groups. The red dots and lines represent the patients in high-risk groups. The green dots and lines represent the patients in low-risk groups. D, Kaplan-Meier survival curves of overall survival among risk stratification groups. E, Univariate Cox regression analyses of clinical factors associated with overall survival. F, Multivariate Cox regression analyses of clinical factors associated with overall survival. G, ROC curve related to clinical factors.

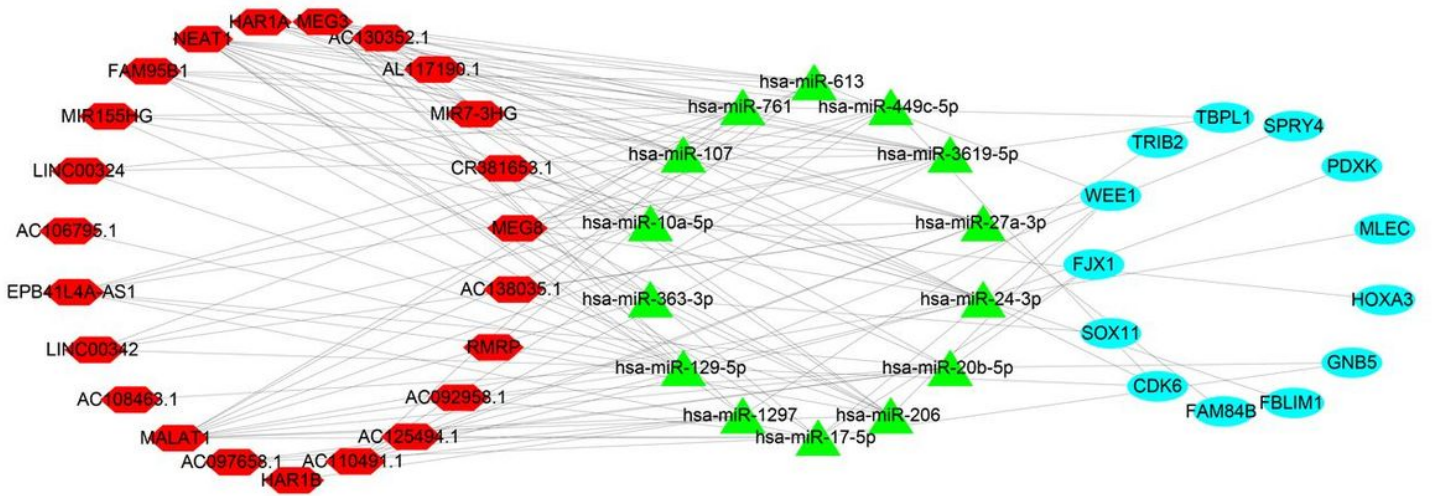


**Figure 7**

The construction of a ceRNA network including 13 mRNAs, 14 miRNAs and 23 lincRNAs. Notes: Red hexagon denotes lincRNA, green triangle represents miRNA, and cyan ellipse represents mRNA.

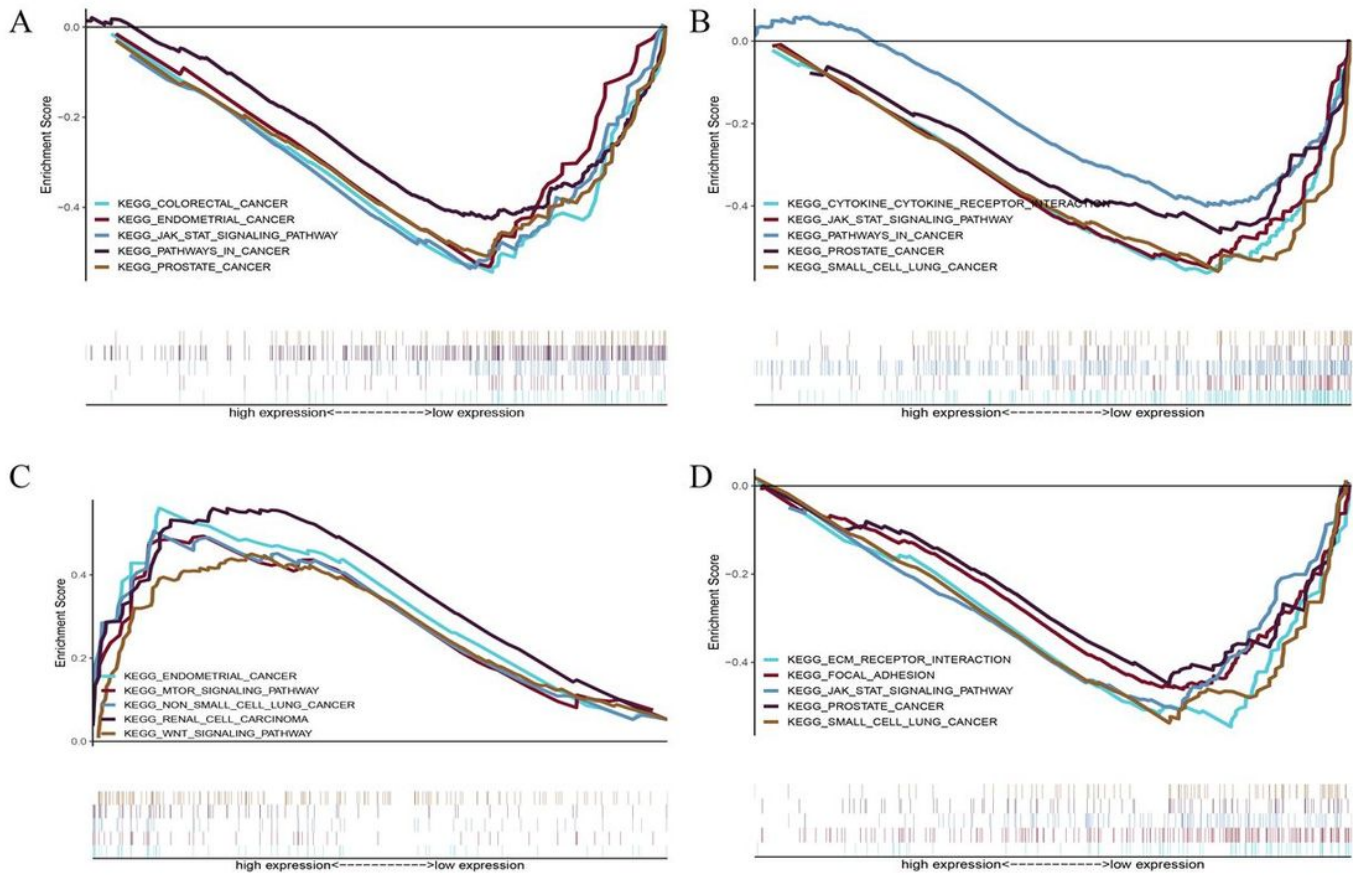


**Figure 8**

Gene set enrichment analysis (GSEA). A, MEG3; B, MIR7-3HG; C, FAM95B1; D, EPB41L4A-AS1.  $P < 0.05$ .